Biophysical Chemistry 8 (1978) 305–315

OPTICAL DIFFRACTION STUDY OF MUSCLE FIBERS
I. A THEORETICAL BASIS

Satoru FUJIME
Mitsubishi-Kasei Institute of Life Sciences, Machida, Tokyo 194, Japan

and

Shigeo YOSHINO
Department of Physics, Faculty of Science, Nagoya University, Nagoya 464, Japan

Received 10 April 1978

We present a simple theoretical model of optical diffraction by striated muscle fibers. The model accounts for (1) changes in diffraction intensity during isometric contraction, (2) spectra of quasielastically scattered light from isometrically contracting muscle, and (3) an electro-optical effect or intensity modulation of diffraction lines by applied electric field. Items (1) and (2) are concerned with the fluctuations of the sarcomere structure during isometric contraction, and item (3) is concerned with the lateral motions of, or the flexibility of, thin filaments in striated muscle at rest.

1. Introduction

A piece of skeletal (or striated) muscle is called a muscle bundle, which consists of many muscle cells (or muscle fibers). A single fiber has a diameter of 50–100 μm and consists of many myofibrils. A fibril has a diameter of the order of 1 μm and consists of many myofilaments called thin and thick filaments. Electron microscopy has shown that the myofilaments pack in the fibril forming a hexagonal lattice. The striations observed by a (polarizing) microscope are due to the periodic change of optical anisotropy, or of the protein concentration, in the fibril. Since this period is of the order of μm, a muscle fiber works as a diffraction grating to visible light.

Optical diffraction studies of muscle fibers have been extensively made by many authors. During the plateau of a smooth tetanus, *no* or *very small* fluctuations of the first order linewidth or zero- to first-order diffraction line spacing are detected [1,2]. The intensity of the first order diffraction line drops siginificantly during isometric contraction [2–4]. One of us studied the intensity drops of diffraction lines and concluded that the intensity drops are mainly due to small random fluctuations of A-band positions around their means [5]. Since, however, the theoretical model in the previous study was too simple to be realistic, we give a more realistic model in section 2, and reconsider the previous experimental results in section 3.

Stimulated by Pecora's work [6], quasielastic light scattering (QELS) has become a powerful tool in studying dynamical properties of (biological) macromolecules in solutions [7]. Thus we try to extend our theory to a dynamical case in order to see a certain aspect of the structure of QELS spectra in section 4.

Skinned fibers of semitendinosus muscle of frogs can be stretched up to 8 μm or more in the sarcomere length (L) and these extremely stretched fibers give quite sharp diffraction patterns. When an electric field (10–100 V/cm) is applied along the fiber axis, intensities of all observable diffraction lines increase (electro-optical effect) [8]. An analysis of the decay process of this excess intensity after turning off the field suggested that the flexural rigidity of thin filaments is $2 \sim 3 \times 10^{-17}$ dyn cm^2. A theoretical basis of this phenomenon is also presented in section 5, and a further experimental study along the lines of the present theory will be given in a subsequent paper. The physical principles included in the theory of this electro-optical effect are very similar in many respects to those of tran-

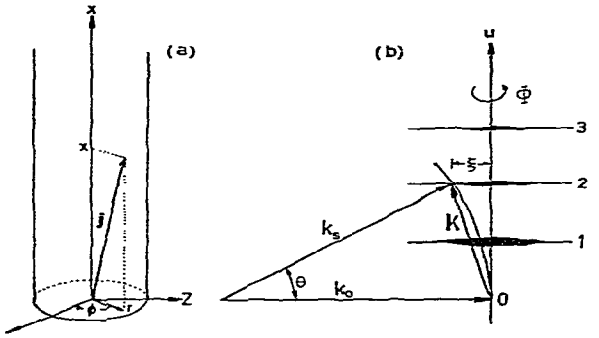

Fig. 1. Geometries in the real (a) and reciprocal (b) space.

sient electric birefringence or the Kerr effect [9]. The essential difference lies in that the effect comes from interference of scattered light in the former and from optical anisotropy of solution as wholes in the latter.

2. Optical diffraction by muscle fibers

2.1. Diffraction intensity

Let us consider a smooth cylinder whose radius and length are R and l respectively. Location in the cylinder is specified by the vector j whose cylindrical coordinates are denoted by r, ϕ and x (fig. 1). The scattering vector $K = k_s - k_0$ ($|K| = (4\pi/\lambda)\sin(\theta/2)$, λ the wavelength of incident light in the fiber and θ the scattering angle) has also the cylindrical coordinates ξ, Φ and u. The scattered field from the cylinder is given by [10]

$$e(K) = C\int_0^l n(x)\,e^{iux}\,dx\int_0^R\int_0^{2\pi} e^{i\xi r\cos(\phi-\Phi)}\,r\,dr\,d\phi, \quad (1)$$

where C is a proportionality constant (hereafter we put $C=1$), and $n(x)$ is the refractive index. Noting that $n(x)$ has period L (i.e., $l = NL$, where L is the sarcomere length and N is the number of unit cells), we have the intensity expression

$$i(K) = |e(K)|^2$$

$$= (\pi R^2)^2\,[2J_1(\xi R)/\xi R]^2\,L(u)|F(u)|^2 \quad (2)$$

where

$$F(u) = \int_0^L n(x)\,e^{iux}\,dx, \qquad L(u) = \frac{\sin^2(uLN/2)}{\sin^2(uL/2)}, \quad (3)$$

and $J_1(x)$ is the Bessel function of the first order. The maxima in the intensity function occur along the u-axis at $u_n = 2\pi n/L$, where n is an integer (diffraction order index) specifying each maximum.

To consider the simplest model of a muscle fiber (or a bundle), we assume that the cylindrical fiber consists of many identical fibrils in near register. The departures from perfect matching between fibrils are supposed to be due to random minor displacements of the fibrils as wholes in the directions parallel with and perpendicular to the fiber axis. The fiber has a radius R_0 while each fibril has a radius R ($R_0 \gg R$). Each fibril, if independent of each other, would diffract according to eq. (1). It is necessary, however, to take account of phase relations of the scattering by different fibrils; $I(u_n, \xi) = i(u_n, \xi)\,\Psi(u_n, \xi)$, where $I(u_n, \xi)$ is the intensity for the fiber and $\Psi(u_n, \xi)$ is the structure factor taking account of the number $(R_0/R)^2$ and the arrangement of fibrils relative to one another. Based on a simple model, the factor $\Psi(u_n, \xi)$ has been calculated [10]. However, this factor is very model dependent, and we do not yet have a reliable form of this factor for a muscle fiber [11].

2.2. Unit cell structure factor

Since $n(x)$ is proportional to the density of proteins in the unit cell (or in a sarcomere), we assume the functional form on $n(x)$ as shown in fig. 2. Then we have

$$F(u) = f_I(u) + \exp(iuL/2)\,f_A(u) \quad (4)$$

or since $u_n = 2\pi n/L$,

$$F(u_n) = f_I(u_n) + (-1)^n f_A(u_n). \quad (5)$$

Apart from a proportionality constant common to both f_I and f_A, they are given by

$$f_I(u_n) = (n_I^0 2a)\,S(2\pi na/L) + (n_Z^0\Delta)\,S(\pi n\Delta/L), \quad (6)$$

$$f_A(u_n) = (n_A^0\hat{b})\,S(\pi n\hat{b}/L) + (n_M^0\delta)\,S(\pi n\delta/L), \quad (7)$$

where $\hat{b} = (b + b')/2$, $b - b' \ll L$ and $S(X) = (\sin X)/X$. Table 1 shows the protein concentrations (in %) given in [12] and those assumed in our calculation. Putting $n_I^0 2a/\pi$ to be unity, we calculated both f_I and f_A as functions of n and L (fig. 3).

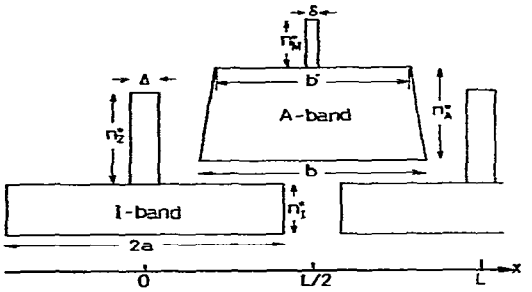

Fig. 2. Functional form of $n(x)$ (cf. table 1).

3. Change in diffraction intensity during isometric contraction

The structure factor $\Psi(u_n, \xi)$ is model dependent, so that the quantitative interpretation of the diffraction intensity is very difficult. Qualitatively speaking, however, the intensity expression

$$I(u_n, \xi) = \Psi(u_n, \xi)\,(\pi R^2)^2$$

$$\times\,[2J_1(\xi R)/\xi R]^2 L(u_n)|F(u_n)|^2, \qquad (8)$$

contains factors due to various imperfections of the fiber structure; effects due to small variations (δL) in the sarcomere length through $L(u_n)$, those due to imperfect register of fibrils through $\Psi(u_n, \xi)$ and those due to changes in the unit cell structure through $F(n_n)$.

Except at $L = 3\ \mu$m, intensities of all observable diffraction lines drop significantly on isometric stimulation [5]. Thus the increase of δL and/or imperfect register during isometric contraction will be possible origins of the intensity drops. These possibilities, however, are not considered to be the most important ones, because *no* or very *small* intensity drop of the second order line is observed at $L = 3\ \mu$m, where intensities of the first- and the third-order lines drop significantly [5]. Therefore the above equation suggests that, during isometric contraction, the value of $|F(u_n)|^2$ changes depending on both n and L. In this connection, we have proposed the importance of the "Debye-Waller" factor, M, in the interpretation of the intensity drops; instead of eq. (5), we have proposed

$$F(u_n) = f_I(u_n)\,e^{-M_I} + (-1)^n f_A(u_n)\,e^{-M_A}, \qquad (9)$$

$$M_\alpha = (1/2)\,\langle \delta x_\alpha^2 \rangle u_n^2 \qquad (\alpha = \text{A or I}), \qquad (10)$$

where $\langle \delta x_\alpha^2 \rangle$ is the mean square amplitude of the axial fluctuations of α-bands around their lattice points. It should be noted that the fluctuations $\langle \delta x_\alpha^2 \rangle$ in the above equation are the *excess* ones during isometric contraction, i.e., the dynamic and/or static disordering of the lattice points at the resting state, if any, is assumed to be incorporated into the scattering factors f's. As shown in appendix 1, $\langle \delta x_\alpha^2 \rangle$ is proportional to the tension F_0, it depends on the sarcomere length.

The solid line (1) in fig. 4 is a qualitative drawing of the intensity change of the first order line [2]. To explain this behaviour on the basis of eq. (9);

$$I(u_1)/I(u_1)_{\text{at rest}} = (f_A\,e^{-M_A} - f_I\,e^{-M_I})^2/(f_A - f_I)^2 \qquad (11)$$

we have several possibilities:

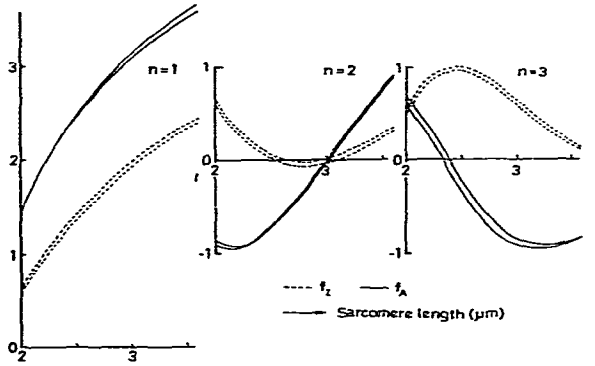

Fig. 3. Scattering form factors f_I and f_A against the sarcomere length L. Dual lines depict possible domain of variations, determined by the distribution of quantities in table 1, within a reasonable limit.

Table 1
Concentration of protein in a myospace

	Huxley and Hanson [12] concentration (%)	Present concentration (%)	Density (arb.) [a]
$n_I^0 \cdot 2a$	36	36	$n_I^0 = 18$
$n_A^0 \cdot \hat{b}$	55	55	$n_A^0 = 36.7$
$n_Z^0 \cdot \Delta$	6	7.2	$n_Z^0 = 36$
S-protein	3	0	
M-protein	–	1.8	$n_M^0 = 18$

[a] $a = 1\ \mu$m, $\hat{b} = 1.5\ \mu$m, $\Delta = 0.2\ \mu$m and $\delta = 0.1\ \mu$m.

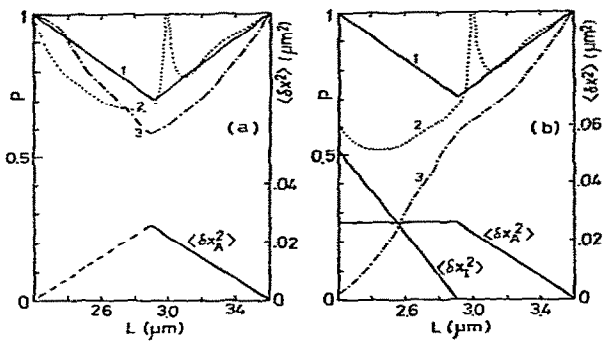

Fig. 4. Estimates of $\langle \delta x_A^2 \rangle$ and $\langle \delta x_I^2 \rangle$ from the model to explain the experimental results of intensity drops for the first three diffraction lines during isometric contraction (see text). The solid line ($n=1$) is from the result of [2]. The dotted lines (2 and 3) are the predicted changes for the second and third lines respectively. $P \equiv I(u_n)/I(u_n)_{\text{at rest}}$.

(a) $M_A = M_I = M$. This case is improbable, because $I(u_1)/I(u_1)_{\text{at rest}} = e^{-2M} = 0.7$ at $L = 2.9$ μm means $M = 0.18$ or $\langle \delta x^2 \rangle = (9\ \mu\text{m})^2$. (b) $M_A < M_I$. Except for $L \leqslant 2.3$ μm (see below), this case is immediately excluded, because $f_A > f_I > 0$ for $n = 1$ over the range of L of the present interest. (c) $M_A > M_I \geqslant 0$. This case may be plausible, at least, at $L \geqslant 2.9$ μm. To explain the experimental result, it is sufficient to assume the value of $\langle \delta x_A^2 \rangle$ shown in fig. 4a. At $L = 2.9$ μm, $\langle \delta x_A^2 \rangle$ is only $(0.17\ \mu\text{m})^2$. The M_I value may not be zero. But M_I values at around $L = 3$ μm might be very small, because $f_A(u_2) = 0$ at $L = 3$ μm. Combining experimental results on the first order line intensity [2] and the second-order line intensity [5] with the present theoretical model, it is reasonable to conclude that $M_A \geqslant M_I \approx 0$ at $L \geqslant 2.9$ μm or, at least, at $L = 3$ μm. This supports our previous conclusion.

But the assumption of $M_A > M_I \approx 0$ encounters a difficulty at $L \leqslant 2.9$ μm, because the value of M_A must decrease as L decreases (the dashed line in fig. 4a), although tension still increases as L decreases. The simplest model to avoid this difficulty may be as follow: At $L \geqslant 2.9$ μm, $M_A > M_I \approx 0$ as stated before. At $L \leqslant 2.9$ μm, M_A values remain constant or slightly increase as L decreases, whereas M_I values increase as L decreases (fig. 4b). The expected behaviour on the intensity drops of the second- and third-order lines is also shown in fig. 4.

4. Intensity fluctuation spectroscopy of muscle fibers during isometric contraction

In order to see a relation between results of static [2–5] and dynamic [13,14] measurements, a simple extension of the above consideration is made. Our present aim is to show the fact that a simple physical model can naturally predict the functional form of the correlation function compatible with the experimental. For simplicity of algebra, the following is restricted only to a simple lattice, i.e., the unit cell has only one lattice point, instead of two lattice points for A- and I-bands. (Extension to a complex lattice is very easy under some restricted conditions.)

According to the elementary theory of X-ray diffraction, we have [15]

$$I(u) = f^2\, e^{-2M} L(u) + f^2 N e^{-2M}(e^{2M} - 1), \qquad (12)$$

where $f^2 = |F(u)|^2 [2J_1(\xi R)/\xi R]^2$. The decrease of the intensity of diffraction lines by the factor $\exp(-2M)$ is compensated by the increase of the background intensity. Extension of eq. (12) to the dynamic case is straightforward and we have

$$I(u, \tau) = f^2 e^{-2M} L(u) + f^2 N e^{-2M} [e^{2M\Phi(\tau)} - 1] \quad (13)$$

$$\Phi(\tau) = \langle \delta x(t)\, \delta x(t+\tau) \rangle / \langle \delta x^2 \rangle = \begin{cases} 1 & \text{as } \tau \to 0 \\ 0 & \text{as } \tau \to \infty \end{cases} \quad (14)$$

where we assumed no correlation of fluctuations between lattice points in different cells, i.e., $\langle \delta x_j \delta x_k \rangle = \langle \delta x^2 \rangle \delta_{jk}$. In the following, we only consider the case of $u \neq u_n$, so that we have $I(u, \tau) = f^2 N e^{-2M} [e^{2M\Phi(\tau)} - 1] \approx f^2 N e^{-2M} 2M\Phi(\tau)$ (for small M). The theory of intensity fluctuation spectroscopy of laser light [7] shows that $\langle I(u,0)\, I(u, \tau) \rangle = I(u)^2 + |I(u, \tau)|^2$, or in the normalized form, $g^{(2)}(\tau) = \langle I(u,0)\, I(u, \tau) \rangle / I(u)^2 = 1 + |\Phi(\tau)|^2$. Inserting eq. (A.3) in appendix 1 into the above equation, we have

$$g^{(2)}(\tau) = 1 + \frac{1}{1-A} [e^{-2q\tau} - A e^{-2q\tau/A}], \qquad (15)$$

where $A = 2A' \leqslant 0.1$ is assumed. Although the above consideration of $g^{(2)}(\tau)$ is concerned with one simple model of many possible ones [14], it is noteworthy that the functional form of the experimental correlation function [13] is quite naturally derived under simple assumptions.

The present model, however, cannot explain all ex-

perimental findings. For example, the $g^{(2)}(\tau)$ was observed even on the zero-order diffraction line [13]. We also confirmed this. In the present framework of the theory, however, the axial movements do not affect the intensity of the zero-order line because $M = 0$ for $u = 0$. However, if we consider the fact that the phase retardation of the beam after passing through a fibril depends on the local index of refraction $n(x)$ and varies with time in a manner characteristic of the axial motions of A- and I-bands, the intensity of the zero-order line is expected to vary with time as a result of phase modulation. This effect will also work at all u-values including $u = u_n$. At present, however, we cannot formulate the $g^{(2)}(\tau)$ due to this effect explicitly because of the lack of knowledge of the averaging procedure with respect to the fiber structure just as in the case of formulating $\Psi(u_n, \tau)$ discussed before.

5. Electro-optical effect of muscle fibers

In a previous paper [8], the electro-optical effect in muscle fibers was interpreted as due to the bending motion of thin filaments as a result of the interaction between electric dipole moments of thin filaments and the external electric field. If this interpretation is valid, we can observe the contribution from the second order mode of the bending motion to the electro-optical effect of muscle fibers under a suitable condition. To see this effect, we extend our previous theory to a more general form. In the following, we ignore any sophisticated problem such as interfilament, hydrodynamic and electrolytic interactions.

5.1. Refractive index of myofibrils under the influence of an electric field

In extremely stretched fibers where there is no overlap between thin and thick filaments, packing of the thin filaments becomes loose because of the repulsive force between them, and because of their flexibility (fig. 5a). Using the notation in fig. 5, we have the functional form of the refractive index of the I-band as ($|p(x)| \ll 1$)

$$n_I^{(a)}(x) = n_I^0[1 + p(x)]^{-2} \approx n_I^0[1 - 2p(x)]. \tag{16}$$

Then we have

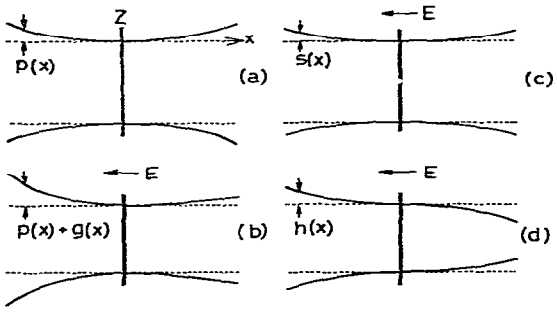

Fig. 5. Schematic representation showing the effect of applied electric field on thin filaments (modified version of fig. 11 in [8]). (a) $E = 0$. $p(x)$ represents the bending of filaments due to repulsive force between them. $p(x) = p(-x) \ll 1$. (b) $E \neq 0$. $g(x)$ represents the effect of applied field E on the electric dipole moments on the filaments, and is assumed to be a sum of $h(x, t)$ and $s(x, t)$. (c) An assumed form of $s(x, t) = s(-x, t)$, and (d) an assumed form of $h(x, t) = -h(-x, t)$.

$$f_I^{(a)}(u) = f_I(u) - 4n_I \int_0^a p(x) \cos(ux)\, dx, \tag{17}$$

$$F^{(a)}(u_n) = f_I^{(a)}(u_n) + (-1)^n f_A(u_n), \tag{18}$$

and

$$I^{(a)}(u_n) = |F^{(a)}(u_n)|^2, \tag{19}$$

where $f_I(u)$ and $f_A(u)$ are given by eqs. (6) and (7) respectively. [Correction by the radial shape factor is negligibly small.] When an electric field is applied, the packing of thin filaments on one side of Z-line becomes denser and that on the other side looser as shown in fig. 5b [8]. In this case we have

$$n_I^{(b)}(x) = n_I^0[1 + p(x) + g(x, t)]^{-2}$$

$$\approx n_I^{(a)}(x) - 2n_I^0 g(x, t). \tag{20}$$

Here we can put without loss of generality

$$g(x, t) = h(x, t) + s(x, t), \tag{21}$$

where $h(x, t)$ and $s(x, t)$ are odd and even functions of x respectively (see fig. 5c and d). Then we have

$$F^{(b)}(u_n) = F^{(a)}(u_n) - \Delta f_I'(u_n, t) - i\Delta f_I(u_n, t), \tag{22}$$

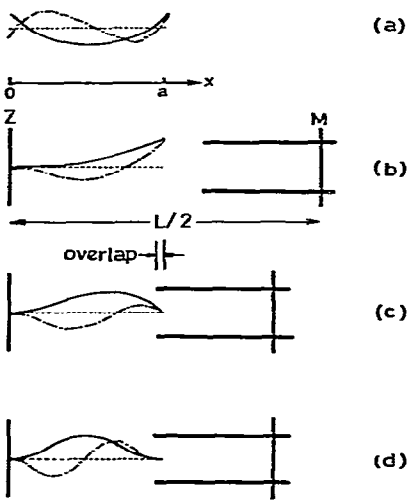

Fig. 6. Schematic representation of the model. M: M-line and Z: Z-line. (a) filaments in solution, (b) muscle fiber without overlap, (c) and (d) rigor muscle fiber with slight overlap. One end of the thin filaments is assumed to be hinged in (c) and fixed in (d). Thin filaments are drawn according to the functional forms of $Q(1,x)$ (——) and $Q(2,x)$ (–·–).

$$f_1(u,t) = 4n_1^0 \int_0^a h(x,t) \sin(ux)\, dx, \tag{23}$$

$$f_1'(u,t) = 4n_1^0 \int_0^a s(x,t) \cos(ux)\, dx. \tag{23'}$$

Now we have

$$I^{(b)}(u_n,t) = I^{(a)}(u_n) + \Delta I_1(u_n,t) + \Delta I_2(u_n,t), \tag{24}$$

where

$$\Delta I_1(u_n,t) = -2F^{(a)}(u_n)\Delta f_1'(u_n,t) + [\Delta f_1'(u_n,t)]^2, \tag{25}$$

$$\Delta I_2(u_n,t) = [\Delta f_1(u_n,t)]^2, \tag{26}$$

are the excess intensity induced by the applied field. The same relations as those considered above also hold for the case where there is a slight overlap between thin and thick filaments, provided that appropriate forms of $p(x)$, $h(x,t)$ and $s(x,t)$ are assumed.

5.2. Motion of a flexible rod

The bending motion of a rod (fig. 6) in a viscous medium is expressed by [8,16,17]

$$\zeta(\partial r/\partial t) + \epsilon(\partial^4 r/\partial x^4) = F(x,t), \tag{27}$$

where ζ is the friction constant per unit length of, and ϵ the flexural rigidity of, the rod, and $F(x,t)$ is the force acting on the rod. By mode expansion

$$r(x,t) = \sum_k q(k,t)\, Q(k,x), \tag{28}$$

$$F(x,t) = \sum_k B(k,t)\, Q(k,x), \tag{28'}$$

eq. (27) becomes

$$\zeta \dot{q}(k,t) + \lambda_k q(k,t) = B(k,t), \tag{29}$$

$$\epsilon[d^4 Q(k,x)/dx^4] = \lambda_k Q(k,x), \tag{30}$$

where λ_k is the separation constant. To solve the eigenvalue problem, eq. (30), the following four cases are considered:

(a) Both ends of the rod are free (fig. 6a) [16];

$$\lambda_k = \epsilon[(k + 1/2)\pi/a]^4 \qquad (k = 1,2,3,\ldots). \tag{31}$$

(b) One end is fixed and the other end is free (fig. 6b) [8];

$$\lambda_1 = \epsilon[0.6\pi/a]^4, \tag{32}$$

$$\lambda_k = \epsilon[(k - 1/2)\pi/a]^4 \qquad (k = 2,3,4,\ldots).$$

(c) One end is fixed and the other end is hinged (fig. 6c);

$$\lambda_k = \epsilon[(k + 1/4)\pi/a]^4 \qquad (k = 1,2,3,\ldots). \tag{33}$$

(d) Both ends are fixed (fig. 6d);

$$\lambda_k = \epsilon[(k + 1/2)\pi/a]^4 \qquad (k = 1,2,3,\ldots). \tag{34}$$

The schematic representation of the functional forms of $Q(k,x)$ are shown in fig. 6 for $k = 1$ and 2.

To solve eq. (29), we consider:

(1) Applied field in a square form (see appendix 2);

$$B(k,t) = E_k \quad \text{for } -T \leqslant t \leqslant 0, \quad \text{and} = 0 \text{ otherwise.} \tag{35}$$

In this case we have

$$q(k,t) = \exp(-t/\tau_k) \int_{-\infty}^{t} B(k,s) \exp(s/\tau_k)\, ds \qquad (36)$$

$$= E_k \tau_k [1 - \exp(-T/\tau_k)] \exp(-t/\tau_k), \qquad (37)$$

$$\tau_k = \zeta/\lambda_k. \qquad (38)$$

(2) Applied field in a sinusoidal form;

$$B(k,t) = E_k \cos(\omega t). \qquad (39)$$

In this case we have from eq. (36)

$$q(k,t) = E_k \tau_k \cos(\phi_k) \cos(\omega t - \phi_k), \qquad (40)$$

$$\phi_k = \tan^{-1}(\omega \tau_k). \qquad (41)$$

5.3. Modulation of diffraction intensity by electric field

Our basic assumption about the electro-optical effect of a muscle fiber is equivalent to putting

$$h(x,t) \propto r(x,t) = \sum_k q(k,t)\, Q(k,x) \quad \text{for } x \geqslant 0. \qquad (42)$$

The function $s(x,t)$ in eq. (21) has been introduced in order to take account of a possible "asymmetric" effect of the applied field; for example, loose packing of thin filaments would occur more easily than dense packing. In the absence of an offsetting field which acts as a bias field, $s(x,t)$ does not depend on the polarity of the applied field. In the presence of an offsetting field, on the other hand, it depends on the polarity of the applied field. For simplicity of algebra, we tentatively assume here

$$s(x,t) \propto \eta \sum_k |q(k,t)| Q(k,x) + \beta \sum_k q(k,t)\, Q(k,x) \quad \text{for } x \geqslant 0. \qquad (43)$$

From the above assumptions, we have from eq. (23)

$$\Delta f_1(u,t) = 4n_1^0 \sum_k A_k(u)\, q(k,t), \qquad (44)$$

$$\Delta f_1'(u,t) = 4n_1^0 \sum_k A_k'(u) [\eta |q(k,t)| + \beta q(k,t)], \qquad (45)$$

$$\begin{Bmatrix} A_k(u) \\ A_k'(u) \end{Bmatrix} = \int_0^a Q(k,x) \begin{Bmatrix} \sin(ux) \\ \cos(ux) \end{Bmatrix} dx, \qquad (46)$$

where a proportionality constant common to both eqs. (42) and (43) is omitted in eq. (46).

For a square field, the offsetting field considered above has no meaning. Putting β in eq. (45) to be zero, we have

$$\Delta I_1(u_n,t) = -8n_1^0\, \eta F^{(a)}(u_n) \sum_k P_k \exp(-t/\tau_k), \qquad (47)$$

$$\Delta I_2(u_n,t) = [4n_1^0 \sum_k R_k \exp(-t/\tau_k)]^2, \qquad (48)$$

where the term proportional to η^2 is neglected in eq. (47), and

$$\begin{Bmatrix} P_k \\ R_k \end{Bmatrix} = E_k \tau_k [1 - \exp(-T/\tau_k)] \begin{Bmatrix} A_k'(u) \\ A_k(u) \end{Bmatrix}. \qquad (49)$$

In this case, a cumulant expansion technique is applicable in the analysis of experimental data [18]. In the extreme case of $\Delta I_1 \gg \Delta I_2$, or very large value of $\eta F^{(a)}(u_n)$, the initial decay rate is given by

$$(1/\tau)_1 \simeq [(1/\tau_1)P_1 + (1/\tau_2)P_2]/[P_1 + P_2]. \qquad (50)$$

On the other hand, in the case of $\Delta I_2 \gg \Delta I_1$, or of very small values of η and/or $F^{(a)}(u_n)$, the initial decay rate is given by

$$(1/\tau)_2 \simeq [(1/\tau_1)R_1 + (1/\tau_2)R_2]/[R_1 + R_2]. \qquad (51)$$

The sign "$\simeq$" is introduced in eqs. (50) and (51) since we consider only the $k = 1$ and 2 modes. Note that $(1/\tau)_1 \neq (1/\tau)_2$ because $A_k' \neq A_k$. The $(1/\tau)$ versus T relations are shown in fig. 7.

Taking the origin of time at $-T$ and omitting the trivial factor $4n_1^0$ in the following discussion, we have from eqs. (48) and (49)

$$\Delta i_R(t) = \sum_k E_k A_k \tau_k [1 - \exp(-t/\tau_k)], \qquad T \geqslant t \geqslant 0, \qquad (52)$$

$$\Delta i_D(t) = \sum_k R_k \exp[-(t-T)/\tau_k], \qquad t \geqslant T, \qquad (53)$$

$$\Delta i(t) = \Delta i_R(t) + \Delta i_D(t), \qquad t \geqslant 0, \qquad (54)$$

where suffixes R and D mean *rise* and *decay* respectively. Now it holds that

$$\sum_k E_k A_k \tau_k = \frac{1}{T}\int_0^\infty \Delta i(t)\,dt. \tag{55}$$

Since $\tau_1/\tau_2 = 40$ and $E_1A_1/E_2A_2 = 9$ at $L = 7$ μm for model (b) in fig. 6, from eqs. (52) and (53) we have for $T \geqslant \tau_1$

$$y(t) = E_1A_1\tau_1\exp(-t/\tau_1), \qquad T \geqslant t \geqslant 0, \tag{56}$$

$$\Delta i_D(t) = [\exp(T/\tau_1) - 1]\,y(t), \qquad t \geqslant T. \tag{57}$$

Then the single-exponential decay rates of $y(t)$ and $\Delta i_D(t)$ should coincide with each other, provided that an induced moment has *no appreciable* effect on $y(t)$.

For a sinusoidal field, $\Delta I_1(u_n, t)$ has a complicated form. Since $|\cos(x)| = (2/\pi) + (4/3\pi)\cos(2x) - (4/15\pi)\cos(4x) + \ldots$, we have the time dependent part of $\Delta I(u_n, t) = \Delta I_1(u_n, t) + \Delta I_2(u_n, t)$ of the present interest as

$$\Delta I(u_n, t) \simeq -B_\omega \cos(\omega t - \phi_\omega) \tag{58}$$

$$-\hat{B}_{2\omega}\cos(2\omega t - 2\hat{\phi}_{2\omega}) + B_{2\omega}\cos(2\omega t - 2\phi_{2\omega}),$$

where the sign "$\simeq$" is introduced because we consider only $k = 1$ and 2 modes and because we neglect the terms proportional to η^2 and $\eta\beta$, and

$$\begin{Bmatrix} V_k \\ U_k \end{Bmatrix} = E_k\tau_k\cos(\phi_k)\begin{Bmatrix} A_k(u) \\ A'_k(u) \end{Bmatrix}, \tag{59}$$

$$B_\omega = 8n_I^0\beta F^{(a)}(u_n)[U_1^2 + U_2^2 + 2U_1U_2\cos(\phi_1 - \phi_2)]^{1/2}, \tag{60}$$

$$\hat{B}_{2\omega} = \frac{32}{3\pi}n_I^0\eta F^{(a)}(u_n)[U_1^2 + U_2^2 + 2U_1U_2\cos(2\phi_1 - 2\phi_2)]^{1/2}, \tag{61}$$

$$B_{2\omega} = 8(n_I^0)^2[V_1^2 + V_2^2 + 2V_1V_2\cos(\phi_1 - \phi_2)], \tag{62}$$

$$\phi_\omega = \tan^{-1}\left[\frac{U_1\sin(\phi_1) + U_2\sin(\phi_2)}{U_1\cos(\phi_1) + U_2\cos(\phi_2)}\right], \tag{63}$$

$$\hat{\phi}_{2\omega} = \frac{1}{2}\tan^{-1}\left[\frac{U_1\sin(2\phi_1) + U_2\sin(2\phi_2)}{U_1\cos(2\phi_1) + U_2\cos(2\phi_2)}\right], \tag{64}$$

$$\phi_{2\omega} = \tan^{-1}\left[\frac{V_1\sin(\phi_1) + V_2\sin(\phi_2)}{V_1\cos(\phi_1) + V_2\cos(\phi_2)}\right]. \tag{65}$$

Note again that $\phi_\omega \neq \phi_{2\omega}$ at a higher frequency region because $A'_k \neq A_k$. The ϕ versus ω relations are shown in fig. 8. The ϕ_ω versus ω relation can be measured by use of a lock-in detector in its ω-mode, and the $\phi_{2\omega}$ versus ω relation in its 2ω-mode (or its harmonics mode).

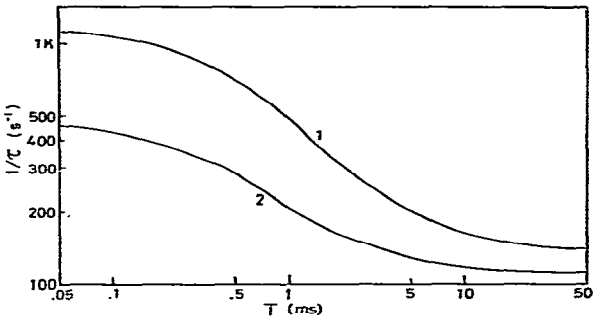

Fig. 7. The $(1/\tau)$ versus T relations for the first order diffraction line. $\tau_1 = 10$ ms and $\tau_1/\tau_2 = 40$ for model (b) and $L = 7$ μm. 1: $(1/\tau)_1$ and 2: $(1/\tau)_2$. (See appendix 3).

6. Discussion

6.1. *Fluctuations of sarcomere structure*

In a previous paper [5], we ignored the contribution from Z- and M-lines to the structure factor $F(u)$. Due to this, we assumed the ratio n_I^0/n_A^0 to be 0.1, in order to explain the extinction of the second order re-

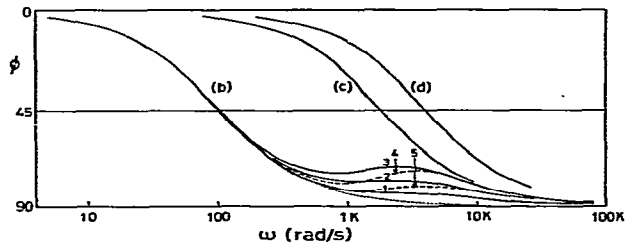

Fig. 8. The ϕ_ω versus ω and $\phi_{2\omega}$ versus ω relations for the first order diffraction line. (b), (c) and (d) correspond to models (b), (c) and (d) in fig. 6 respectively. $\tau_1 = 10$ ms and $\tau_1/\tau_2 = 40$ for model (b). In model (b), 1: $\phi_{2\omega}$ at $L = 4$ and 7 μm (deviation $\leqslant 1°$), 2: ϕ_ω at $L = 7$ μm, 3: ϕ_ω at $L = 4$ μm, 4: $\hat{\phi}_{2\omega}$ at $L = 4$ μm, 5: $\hat{\phi}_{2\omega}$ at $L = 7$ μm, and (····): $\phi = \tan^{-1}(\omega\tau_1)$. The deviation of curves 1 ~ 5 from the dotted line is due to the contribution from the $k = 2$ mode. In models (c) and (d), $L = 3.5$ μm, $\phi_\omega = \phi_{2\omega}$ in the frequency range of the present interest, and the contribution from the $k = 2$ mode is negligibely small for model (c) and zero for model (d) because of $E_2 \approx 0$ for (c) and zero for (d) (see appendices 2 and 3).

flection at $L = 3$ μm. This is really unnatural. The present version of the model, although it still has the unsolved factor $\Psi(u_n, \xi)$, overcame this difficulty and confirmed the validity of the main conclusion of the previous study. The statements in *Related problem* at the last part of [5], however, seems to be incorrect, and we are inclined to think that the fluctuations of the sarcomere structure are something like those shown in fig. 4b. We are now elucidating this problem from both static and dynamic measurements.

From the experimental results of $A \simeq 0.1$, $\tau_{1/2} \simeq 1$ ms [13] and $\langle \delta x^2 \rangle \simeq (0.2\ \mu\text{m})^2$ [5], and from the reported values of $F_0 = 3.5$ kg/cm^2, $\sigma = 1 \times 10^{-6}$ dyn and $\bar{n} = 4 \times 10^4$ per half sarcomere of a fibril [14], our theory gives $\kappa \simeq 10$ dyn/cm and $\gamma \simeq 2 \times 10^{-3}$ dyn/cm·s. It is not clear to what the elastic component having the force constant of $\kappa \simeq 10$ dyn/cm corresponds. However, the estimated value of $\gamma \simeq 2 \times 10^{-3}$ dyn/cm·s is close to $\gamma = 2.2 \times 10^{-3}$ dyn/cm·s estimated from the free draining model, i.e., the γ-value is equal to the product of the friction constant, 2.8×10^{-6} dyn/cm·s, of one thick filament in water and the number, say 800, of thick filaments in a sarcomere of a fibril. This order of magnitude agreement of the γ-values suggests that our model elucidates, at least, qualitatively the relation between intensity drops of diffraction lines of, and QELS spectra of, muscle fibers during isometric contraction. Static and dynamic study of muscle fibers along this line will provide some of basic properties of isometrically contracting muscle.

6.2. Electro-optical effect

In the previous study [8], we only discussed the $k = 1$ mode of the bending motion of thin filaments based on model (b) in fig. 6, and obtained the flexural rigidity of $\epsilon = 2 \sim 3 \times 10^{-17}$ dyn·cm^2. To support the validity of the present model, we must show, at least, the following points.

(1) Since ϵ is a material constant, it does not depend on the sarcomere length. Then, from eqs. (32), (33) and (34), the dispersion frequency ω_1 of the first mode which gives $\phi_{2\omega} = \pi/4$, for example, is about 20 times [in model (c)] or 40 times [in model (d)] higher than that in model (b) (see fig. 8). The boundary conditions for model (c) or (d) will be realized in a *rigor* muscle fiber with a slight overlap between both filaments.

(2) Since the sign of B_ω depends on the diffraction order index n ($F^{(a)}(u_1) < 0$ and $F^{(a)}(u_2) > 0$ for $L \geqslant 3$ μm), we can check the validity of the model by measuring the phase retardation in the ω-mode of the lock-in detector for both the $n = 1$ and 2 diffraction lines.

(3) At shorter durations or higher frequencies of applied field, we can "see" the contribution from the $k = 2$ mode for model (b) as shown in figs. 7 and 8.

(4) In model (c) (and (d)), the contribution from the $k = 2$ mode is expected to be negligibly small because of $E_2 \simeq 0$ (= 0). Although it may be difficult to precisely measure the ϕ_ω versus ω or $\phi_{2\omega}$ versus ω relation at a higher frequency region, this kind of measurements will provide an indication of the validity of the model.

(5) As suggested by eqs. (56) and (57), we can know whether or not an induced moment has an appreciable effect.

In case (1), the theoretical prediction does not depend on the details of the physical model but only on the boundary conditions. In case (2), the theoretical prediction depends on both the diffraction theory and the physical model. In cases (3), (4) and (5), on the other hand, the theoretical predictions strongly depend on the details of the physical model. If these predictions are proved, our model has a firm support, and our experimental technique will become a powerful tool to study some physicochemical and thermodynamic properties of thin filaments *in vivo*. Experimental verification of the present theory as well as some of application of the method will be given in Part II of this series [19].

Appendix 1

In order for the regular structure of sarcomers to be kept, A-bands (and also I-bands) must be connected each other with a spring-like force. We assume the viscoelastic model of fibril shown in fig. 9. Let the friction constant of an A-band be γ. Then the position δx_j of the jth M-line deviating from its mean position (lattice point) will obey the following equation ($j = 1, 2, \ldots, N$)

$$\gamma(\delta \dot{x}_j) - \kappa_A^0(\delta x_{j-1} - 2\delta x_j + \delta x_{j+1}) = F_j(t), \qquad \text{(A.1)}$$

for $\kappa_A^0 \ll \kappa_{A'}$ or

$$\gamma(\delta \dot{x}_j) + \kappa_A(\delta x_j) = F_j(t), \qquad \text{(A.2)}$$

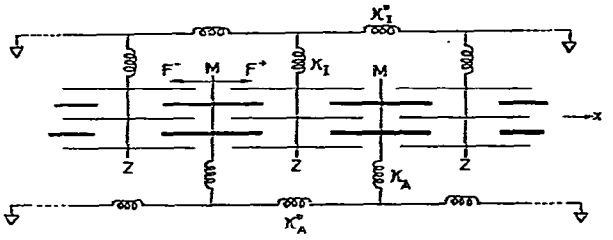

Fig. 9. Viscoelastic model of a fibril. M: M-line, Z: Z-line, κ's spring force constants. Because of the isometric condition, both ends of the fibril are fixed (⊽) where the effect of series elastic components is ignored. F^+ and F^-: forces acting on an M-line.

for $\kappa_A^0 \gg \kappa_A$. The Z-line motion will also obey the same type of equations as above. In the case of eq. (A.1), the lowest mode with the largest amplitude will be given by (boundary conditions; $\delta x_1 = \delta x_N = 0$) $\delta x_j(t) = a \sin[\pi(j-1)/N]\ \xi(t)$ or $\langle \delta x_j^2 \rangle = a^2 \sin^2[\pi(j-1)/N]$ where a is a constant and $\xi(t)$ is the time-dependent part ($\langle \xi(t)^2 \rangle = 1$). The fluctuation is the largest at $j = N/2$. Experimentally speaking, this is probably not the case. Thus we assume eq. (A.2). In this case, δx_j is independent of the suffix j.

In tetanized muscle, there will be a large fluctuating force, $F_j(t)$, due to imbalance of the actin-myosin interaction in half sarcomeres. We assume for tetanized muscle (fig. 9) $F(t) = F^+(t) + F^-(t)$, $F^+(t) = \sigma[\bar{n} + \delta n^+(t)]$ and $F^-(t) = -\sigma[\bar{n} + \delta n^-(t)]$, where σ is the force developed by one actin-myosin connection, $\bar{n}$ the average number of such connections in a half sarcomere of a fibril and δn the fluctuation in n. Then we have $\langle F^+(t) \rangle = -\langle F^-(t) \rangle = F_0/2$ (F_0: contractile force per fibril) and $\langle F(t)\, F(t+\tau) \rangle = 2\sigma^2 \langle \delta n(t)\, \delta n(t+\tau) \rangle$, where no correlation between δn^+ and δn^- is assumed. When we write [20], for simplicity of algebra,

$$\partial n/\partial t = -(f+g)n + g n_0,$$

where f and g are the kinetic constants of the breaking and formation of the actin-myosin connection, respectively, and n_0 the total number of cross-bridges in a half sarcomere, we have $\bar{n} = n_0 g/(f+g)$ and $\langle \delta n(t)\, \delta n(t+\tau) \rangle = \bar{n} \exp(-\Gamma\tau)$ [$\Gamma = f + g$ and $\langle \delta n^2 \rangle = \bar{n}$]. In this model, we have $\langle F(t)\, F(t+\tau) \rangle = (2\sigma^2\bar{n}) \times \exp(-\Gamma\tau)$ or the power spectrum of the fluctuating force of $G(\omega) = 4(2\sigma^2\bar{n})/(\omega^2 + \Gamma^2)$. Then, we have [21,22]

Table 2
Numerical values of coefficients for the first order line. (see eqs. (46) and (A.5)

	Sarcomere length (μm)		
	7.0	4.0	3.5
	Model (b)		Model (c)
A_1	0.468	0.670	0.725
A_2	0.092	0.194	−0.106
A_1'	0.612	0.367	0.307
A_2'	0.447	0.456	0.395
E_1	0.783		0.860
E_2	0.434		0.083

$$\langle \delta x^2 \rangle \Phi(\tau) \equiv \langle \delta x(t)\, \delta x(t+\tau) \rangle$$

$$= \frac{(2\sigma^2\bar{n})}{\pi\gamma^2} \int_{-\infty}^{\infty} \frac{e^{i\omega\tau}}{(\omega^2+p^2)(\omega^2+q^2)}\, d\omega,$$

or

$$\Phi(\tau) = \frac{1}{1-A'} [e^{-q\tau} - A' e^{-q\tau/A'}], \qquad \text{(A.3)}$$

where

$$\langle \delta x^2 \rangle = \frac{2\sigma^2\bar{n}}{\kappa\gamma(p+q)} = \frac{\sigma F_0}{\kappa\gamma(p+q)}, \qquad A' = q/p, \qquad \text{(A.4)}$$

$p = \Gamma$ and $q = \kappa/\gamma$ for $\Gamma > \kappa/\gamma$,

$p = \kappa/\gamma$ and $q = \Gamma$ for $\Gamma < \kappa/\gamma$.

[It must be mentioned that the above formulation of $G(\omega)$ may not be applied to muscle at twitch contraction, where a quasistationary process is not established, and that the model for calculating $\delta n(t)$ should be modernized, for example, to what [23] discussed.]

Appendix 2

We assume that each thin filament has a permanent dipole moment directing from the free end to the Z-line [8]. An induced moment is not considered. For small bending, it holds that $|\partial r/\partial x|^2 \ll 1$, i.e., the angle $\theta(x)$ between the applied electric field and the moment at x is very small. Then the torque to reorient, or the force to bend, the filament is parallel with r and independent of x. In such a case, the kth component of the external force is proportional to

$$E_k = (r/i)\int_0^a Q(k,x)\,\mathrm{d}x. \qquad \text{(A.5)}$$

In models (b) and (c) in fig. 6, $E_2 \neq 0$ because of asymmetric boundary conditions.

Appendix 3

Table 2 shows the numerical values of coefficients E_k, A_k and A'_k used for calculation of $(1/\tau)$ and ϕ in figs. 7 and 8 respectively.

Acknowledgement

We thank Miss S. Chiba for her assistance in machine computation.

References

[1] D.R. Cleworth and K.A.P. Edman, J. Physiol. 227 (1972) 1.
[2] M. Kawai and I.D. Kuntz, Biophys. J. 13 (1973) 857.
[3] D.K. Hill, J. Physiol. 119 (1953) 501.
[4] P.J. Paolini, R. Sabbadiani, K.P. Roos and R.J. Baskin, Biophys. J. 16 (1976) 919.
[5] S. Fujime, Biochim. Biophys. Acta 379 (1975) 227.
[6] R. Pecora, J. Chem. Phys. 40 (1964) 1604.
[7] H.Z. Cummins, in: Photon correlation and light beating spectroscopy, eds. H.Z. Cummins and E.R. Pike (Plenum New York, London, 1973) p. 285
[8] Y. Umazume and S. Fujime, Biophys. J. 15 (1975) 163.
[9] C.T. O'Konski and A.J. Haltner, J. Amer. Chem. Soc. 78 (1956) 3604.
[10] R.S. Bear and O.E.A. Boulduan, Acta Cryst. 3 (1950) 236.
[11] E. Rome, PhD thesis, University London (1967), cited in [13].
[12] H.E. Huxley and J. Hanson, Biochim. Biophys. Acta 23 (1957) 229.
[13] R.F. Bonner and F.D. Carlson, J. Gen. Physiol. 65 (1975) 555.
[14] F.D. Carlson, Biophys. J. 15 (1975) 633.
[15] W.R. James, in: The optical principles of the diffraction of X-ray, (Bell and Sons Ltd, London, 1950) p. 20.
[16] S. Fujime and M. Maruyama, Macromolecules 6 (1973) 237.
[17] R.A. Harris and J.E. Hearst, J. Chem. Phys. 44 (1966) 2595.
[18] D.E. Koppel, J. Chem. Phys. 57 (1972) 4814.
[19] S. Yoshino, Y. Umazume, R. Natori, S. Fujime and S. Chiba, Biophys. Chem. 8 (1978) 317.
[20] A.F. Huxley, in: Progress in biophysics, Vol. 7 (1957) p. 255.
[21] C. Kittel, in: Elementary statistical physics (John Wiley, New York, 1958) p. 147.
[22] M.C. Wang and G.E. Uhlenbeck, Rev. Mod. Phys. 17 (1945) 323.
[23] J. Borejdo and M.F. Morales, Biophys. J. 20 (1977) 315.